01 Aug 1994

Landau-Zener Treatment of Intensity-Tuned Multiphoton Resonances of Potassium

J. Greg Story
Missouri University of Science and Technology, story@mst.edu

D. I. Duncan

Thomas F. Gallagher

Landau-Zener treatment of intensity-tuned multiphoton resonances of potassium

J. G. Story, D. I. Duncan, and T. F. Gallagher
Department of Physics, University of Virginia, Charlottesville, Virginia 22901
(Received 28 February 1994)

When exposed to intense light of ~580 nm, the ground state of K shifts up in energy, passing through two photon resonances with Rydberg states, and finally crossing the two-photon ionization limit. We have used laser pulses of varying duration to study the nature of the population transfer from the ground state to the excited state due to the intensity-tuned resonances encountered during the rising edge of the pulse. A dynamic Floquet approach in which the resonances are treated as avoided crossings of the Floquet energy levels is used to model the population transfer and gives excellent agreement with the data. The model is extended into the strong-coupling regime where the ground state interacts with many excited states simultaneously, and we show that this model can be used to describe multiphoton ionization as a series of avoided crossings with the continuum.

PACS number(s): 32.80.Rm

I. INTRODUCTION

The importance of the intensity-dependent shift of atomic energy levels in multiphoton ionization has been demonstrated by a number of experiments [1–7]. During an intense laser pulse the relative ac Stark shifts of the atomic energy levels may bring the ground state into multiphoton resonance with the excited states [3–7], and the occurrence of these multiphoton resonances has been shown to greatly increase the probability of ionization [4]. In general, the ground-state energy shifts through multiphoton resonance with several excited states on the rising edge of the pulse, and how rapidly the states pass through the resonance is, not surprisingly, important. A natural way of describing the evolution of such a system is to apply the "curve crossing" approach of slow atomic collisions to the Floquet states of the atom in the periodic laser field [8–10]. This approach naturally leads to the conclusion that for very short pulses, resonances encountered in the rapidly changing intensity of the rising edge of the pulse are less important than those encountered near the temporal peak of the pulse, when the intensity changes much more slowly [4,11,12]. In contrast, for long pulses the first resonances encountered can determine the outcome by taking all the population from the ground state.

In a previous paper we briefly discussed a multiphoton excitation and ionization experiment in K and compared the experimentally observed variation of the final state population with laser pulse length to calculations based on the dynamic Floquet model mentioned above [7]. Here we present a more complete description of an expanded set of experiments and the dynamic Floquet model. The paper is organized in the following way. In Sec. II the dynamic Floquet model which is used to analyze the experiment is introduced. In Sec. III the experimental setup is described, and the experimental data are presented. In Sec. IV the Landau-Zener formula used in the dynamic Floquet model is extended to the strong-coupling regime in which the ground state interacts with many states simultaneously, and experimental data are presented which show that the Landau-Zener formalism is still useful in this regime. A theoretical extension to infinitesimal spacing, i.e., the continuum, is presented which suggests an alternative view of multiphoton ionization.

II. THE DYNAMIC FLOQUET MODEL

Figure 1 shows the relevant energy levels of potassium [13]. Also shown in the figure are the two 4*s* Floquet states, corresponding to the one- and two-photon dressed ground states. The essential idea of the Floquet approach is that the energy of any state can be shifted by an integer times the photon energy, so that all states lie in an energy

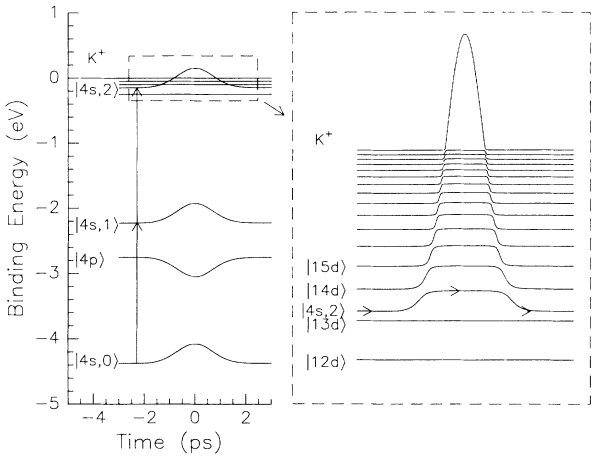

FIG. 1. The relevant energy levels of K are shown along with the one- and two-photon interaction. The states $|4s,1\rangle$ and $|4s,2\rangle$ represent the dressed ground state with one and two photons, respectively. During the laser pulse, interaction between the $|4s,1\rangle$ and $|4p\rangle$ states causes an upward shift of the ground state. An expanded view of the $|4s,2\rangle$ state shows that as the ground-state energy increases, the $|4s,2\rangle$ state passes through a series of anticrossings due to interaction with the *nd* Rydberg series. For a sufficiently large shift, the $|4s,2\rangle$ state crosses into the continuum so that two photons can ionize the ground state.

band spanning $h\nu$. With electric-dipole coupling, even-parity states, which have $Nh\nu$ added to their energies, are coupled to odd-parity states with $(N\pm1)h\nu$ added to their energies. At zero intensity, the dressed states have the energy of the ground state plus an integral number of photons. The energy of the ground state plus one photon lies approximately 0.5 eV above the $4p$ state. As the intensity is increased, the interaction between the $4s$ Floquet state and $4p$ state causes the energy of the $4s$ state to shift upward. This shift can be seen in Fig. 1 as a repulsion between the ground state dressed with one photon and the $4p$ state, due to a laser pulse of 1-ps duration. The energy of the ground state plus two photons, at zero intensity, lies just below the ionization limit. At sufficient intensity the energy of the ground state pulse two photons is shifted above the ionization limit so that two-photon ionization can occur.

The two-photon ionization of the ground state, because of the relatively low order of the process, is easily saturated. For a laser pulse with sufficient intensity to shift the $4s$ Floquet state above the two-photon ionization limit, all atoms in the ground state would be expected to be ionized. However, to reach the ionization limit, the ground state passes through two-photon resonances with the Rydberg states during the rising edge of the laser pulse. These resonances can lead to population trapping in the Rydberg states and thus partial, or in the extreme case, total depletion of the ground state before two-photon ionization can occur. Figure 1 shows an expanded view of the Floquet states near the ionization limit. As the $4s$ Floquet state shifts upward, the two-photon interaction between the ground state and the nd Rydberg states produces a series of avoided crossings between the $|4s,2\rangle$ Floquet state and the Rydberg states. Here $|4s,2\rangle$ denotes the ground state plus two photons. These energy levels are calculated by diagonalizing the adiabatic Floquet energies at each laser intensity for a fixed laser frequency. Only the relative shift between the ground state and the Rydberg states is shown. The ponderomotive shift, which is common to all of the atomic states, is neglected. The inclusion of the ponderomotive shift would raise the energy of all of the states so that Rydberg states would also show a shift during the laser pulse. Only the nd Rydberg states are shown because circular polarization was used in the experiment so that the $|4s,2\rangle$ state interacts only with $l=2$ states. With electric-dipole coupling the ground state is not coupled to other l states. Before the laser pulse, the atoms are in the $4s$ ground state. As the laser pulse turns on, the system moves through the avoided crossings. For a sufficiently rapid increase in intensity and thus rapid passage through the avoided crossings, we would expect the system to evolve diabatically, so that all of the atoms remain in the ground state. For a sufficiently slow increase in intensity, we would expect the system to evolve adiabatically so that after passage through the first avoided crossing (with the $14d$ state in Fig. 1), all of the atoms would be in the excited state. The adiabatic case is shown in Fig. 1 as the solid line with arrows.

The significance of the population of the Rydberg states during the rising edge of the pulse is that the Rydberg states are less likely to be photoionized than the ground state [14–17]. Even though the photoionization of the Rydberg states is a one-photon process, the cross sections for photoionization are small. Since a Rydberg electron must exchange momentum with the ion during photoabsorption to conserve both momentum and energy, the electron can only absorb photons when it is near the core. The Rydberg electron spends the majority of its time at its classical outer turning point, far from the core, where it can not absorb a photon. In contrast, in the ground state the electron is near the core so that, even for a two-photon process, the photoionization probability is relatively large. For two-photon ionization of the $4s$ ground state of K just above the two-photon ionization limit we calculate the cross section to be

$$\sigma_{4s}=1.0\times10^{-47}\ \text{cm}^4\ \text{s} \tag{1}$$

which gives a saturation intensity, for a 1-ps pulse

$$I_s=(\tau_{\text{FWHM}}\sigma_{4s})^{-1/2}=1.1\times10^{11}\ \text{W/cm}^2 \tag{2}$$

at $\lambda=580$ nm. The cross section for one-photon ionization of the $14d$ state is calculated to be

$$\sigma_{14d}=7.5\times10^{-20}\ \text{cm}^2 \tag{3}$$

which gives a saturation intensity, for a 1-ps pulse,

$$I_s=(\tau_{\text{FWHM}}\sigma_{14d})^{-1}=4.6\times10^{12}\ \text{W/cm}^2\ . \tag{4}$$

The saturation intensity is over 40 times greater for the one-photon process from the Rydberg states than the two-photon process from the ground state. The photoionization cross sections scale as n^{-3}, so that the saturation intensity increases for higher Rydberg states. The relative probability of ionization suggests that an atom is more likely to survive a laser pulse which has sufficient intensity to shift the $4s$ Floquet state above the ionization limit if it makes a transition to a Rydberg state during the rising edge of the pulse. The presence of resonances encountered during the rising edge of the pulse can, in this system, result in population trapping and the inhibition of multiphoton ionization.

The probability of remaining in the $4s$ Floquet state after traversing an anticrossing can be obtained using the Landau-Zener formula. For an avoided crossing with a particular n state, the probability is given by [18,19]

$$P_g(n)=\exp\frac{-2\pi V_n^2}{dW/dt}\ , \tag{5}$$

where W is the difference in energy between the $4s$ and nd Floquet energies and V_n is the coupling between the two states. The two-photon coupling between the $4s$ and nd states, in atomic units, is given by

$$V_n=\sum_{n'}\frac{\langle nd|z|n'p\rangle\langle n'p|z|4s\rangle}{\omega_{4sn'p}-\omega}E^2\ , \tag{6}$$

where $\langle nd|z|n'p\rangle$ and $\langle n'p|z|4s\rangle$ are electric-dipole matrix elements, and E is the laser field amplitude with $E^2=(8\pi/c)I$, where I is the laser intensity. The denominator of Eq. (6) is the detuning of the laser from the $4s$-$n'p$ resonances. Equation (6) is written in terms of

linear polarization for simplicity. Circular polarization was used in the experiment so that z is replaced by $(x+iy)/2$. The laser is tuned near the $4s$-$4p$ resonance as can be seen in Fig. 1, and in K, nearly all of the oscillator strength from the $4s$ state is in the $4s$-rp resonance, so that only the $4p$ state has a significant contribution to the two-photon coupling of the $4s$ state to the nd states. The coupling is then given to a good approximation by

$$V_n=\frac{\langle nd|z|4p\rangle\langle 4p|z|4s\rangle}{\omega_{4s4p}-\omega}E^2 . \tag{7}$$

This coupling represents the on resonant, two-photon Rabi frequency, which is the minimum energy separation of the avoided crossings. The only variation of V_n with n is due to the $\langle nd|z|4p\rangle$ matrix element, which scales as $n^{-3/2}$, so the avoided crossing size decreases with n. However, the decrease is slower as a function of n than the spacing between states which decreases as n^{-3}, suggesting that for sufficiently high n, the system no longer passes through isolated avoided crossings. This situation will be considered in Sec. IV. For the present we shall assume the avoided crossings to be isolated, i.e., V_n to be much smaller than the spacing between Rydberg states.

To reach the two-photon ionization limit, the $4s$ Floquet state must pass through an infinite number of avoided crossings. The final population remaining in the $4s$ Floquet state as it crosses the limit is given by

$$P_g=\prod_{n=i}^{\infty}P_g(n) , \tag{8}$$

where i is the first avoided crossing encountered ($n=14$ in Fig. 1). The population given by Eq. (8) represents the percentage of atoms which can undergo two-photon ionization by the laser pulse. If the $4s$ Floquet state is completely depleted, then no atoms can be ionized by two photons. The population in the excited state n_0 after the rising edge of the pulse is given by

$$P_{n_0}=[1-P_g(n_0)]\prod_{n=i}^{n_0-1}P_g(n) \tag{9}$$

which is the probability of making a transition from the $4s$ Floquet state to the n_0 state times the population left in the $4s$ state after traversing all previous avoided crossings.

So far we have only considered the rising edge of the laser pulse. Figure 1 shows that the system passes through the same avoided crossings on the falling edge of the pulse. The avoided crossings traversed on the falling edge will also produce transitions. In particular, consider the fully adiabatic limit in which all of the population is left in the excited state after the first avoided crossing. During the falling edge of a temporally symmetric pulse, all of the population will return to the $4s$ Floquet states as shown by the arrows in Fig. 1. So in the final state of the system, after the laser pulse, all of the atoms are in the ground state except for those atoms which were photoionized from the excited state. Since we saw in the previous discussion that the probability of photoionization is smaller for the excited-state atoms than for the ground-state atoms, the fully adiabatic limit provides a method of shelving the atom during the laser pulse but leaving the system in the ground state after the pulse.

The transition probabilities shown in Eq. (5) are based on the assumption that the energy difference between the $4s$ and nd Floquet states varies linearly with time. It was shown by Rubbmark *et al.* that the Landau-Zener transition probability is a good approximation as long as the energy difference varies approximately linearly over the range of the avoided crossing [20]. In the case where the avoided crossing occurs near the peak of the laser pulse this approximation is not valid. To describe this important case McIlrath *et al.* extended the Landau-Zener method to include the second derivative of the energy separation. Their expression for $P_g(n)$ has the form [12]

$$P_g(n)=\exp\left[\frac{-2\pi V_n^2}{|dW/dt|+\alpha^{-2}|dW^2/dt^2|^{2/3}}\right] , \tag{10}$$

where $\alpha=(1/2\pi)(\frac{4}{3})^{1/3}[\Gamma(\frac{1}{3})]^2$. The correction has a non-negligible effect on the transition probability only when the first derivative is nearly zero. Another case of some interest is one considered by Vrijen, Hoogenraad, and Noordam [21]. Consider an n-photon resonance where n is reasonably large, ~ 6, which is encountered on the rising edge of the pulse. In this case the coupling matrix element can increase more rapidly than the tuning of the levels, so that the levels no longer cross in the usual sense. The standard Landau-Zener formula is clearly inapplicable in this case.

With the expression in Eq. (10), we can calculate the probability of remaining in the $4s$ Floquet state, given the time-dependent shift of the energy levels and the coupling, which both depend on the laser pulse. In our experiment we have a laser pulse with an approximately Gaussian temporal dependence

$$I=I_0\exp(-t^2/\tau^2) \tag{11}$$

where τ is the temporal parameter, which is related to τ_{FWHM}, the full width at half maximum, by $\tau=\tau_{\mathrm{FWHM}}(\ln 2)^{-1/2}$. The rate of change of the intensity is given by

$$\frac{d}{dt}I=\frac{2I}{\tau}[\ln(I_0/I)]^{1/2} , \tag{12}$$

and at the peak of the pulse the second derivative is

$$\frac{d^2}{dt^2}I=\frac{-2I_0}{\tau^2} . \tag{13}$$

The intensity-dependent shift of the $4s$ Floquet state is given by lowest-order perturbation theory, in atomic units, as

$$\Delta=U_p\sum_n\frac{2\omega_{4snp}^3}{\omega_{4snp}^2-\omega^2}|\langle 4s|z|np\rangle|^2 , \tag{14}$$

where ω_{4snp} is the resonant frequency of the $4s$-np transition and ω is the laser frequency. U_p is the ponderomotive energy in atomic units,

$$U_p = \frac{2\pi I}{c\omega^2} . \tag{15}$$

In K virtually all of the oscillator strength from the $4s$ state is in the $4s$-$4p$ transition, so we neglect all other terms in the sum and use the oscillator strength sum rule to give

$$\Delta = U_p \frac{\omega_{4s4p}^2}{\omega^2 - \omega_{4s4p}^2} = 1.3 U_p \tag{16}$$

for the laser frequency of 580 nm used in the experiment. A shift of 1000 cm^{-1} is produced by a laser intensity of 3.8×10^{12} W/cm^2. For a laser tuning near the $4s$-$4p$ resonance, as is the case in this experiment, we can use the rotating-wave approximation, neglecting the negative energy term to give

$$\Delta \cong \frac{V_{4s4p}^2}{4(\omega_{4s4p} - \omega)} , \tag{17}$$

with the interaction between states given by

$$V_{4s4p}^2 = \frac{8\pi}{c} I |\langle 4s|z|4p\rangle|^2 . \tag{18}$$

Equation (17) is the shift obtained by diagonalizing the two-state problem with the $4s$ and $4p$ Floquet states, in the limit that the interaction is much smaller than the energy separation of the states. We can now relate the two-photon interaction V_n given by Eq. (7) to the shift of the ground $4s$ state with the following expression:

$$V_n = 4\Delta_n \frac{\langle 4p|z|nd\rangle}{\langle 4s|z|4p\rangle} , \tag{19}$$

where Δ_n is the shift of the $4s$ Floquet state necessary to bring the $4s$ and nd Floquet states into resonance. Equation (19) shows that the interaction of the $4s$ and nd Floquet states is proportional to the shift of the $4s$ state. The ratio of the dipole moments is given by [22]

$$\frac{\langle 4p|z|nd\rangle}{\langle 4s|z|4p\rangle} = 1.26 n^{-3/2} . \tag{20}$$

The final result for the probability of making a diabatic transition is given by

$$P_g(n) = \exp\left[\frac{-2\pi V_n^2 (\tau/2\Delta_n)\epsilon}{1+\epsilon[\ln(\Delta_{\max}/\Delta_n)]^{1/2}}\right]$$

$$= \exp\left[\frac{-16\pi(1.6) n^{-3}\tau\epsilon}{1+\epsilon[\ln(\Delta_{\max}/\Delta_n)]^{1/2}}\right] , \tag{21}$$

where $\Delta_{\max}$ is the shift of the $4s$ Floquet state at the peak of the laser pulse and $\epsilon = (\Delta_n\tau/3)^{1/3}\pi^{-1}\Gamma^2(\frac{1}{3}) = 1.58(\Delta_n\tau)^{1/3}$. The shift Δ_n is dependent on the initial tuning of the laser. Given the initial tuning and the maximum ac Stark shift of the $4s$ Floquet state, the transition probabilities to all the Rydberg states can be calculated using Eq. (21). In the next section, in which the experiment is described and the data are presented, Eq. (21) will be used to model the population transfer to the Rydberg states during the laser pulse.

III. EXPERIMENTAL APPROACH AND OBSERVATIONS

The experiment was performed by exciting K atoms in an effusive atomic beam with a focused ps dye laser beam. A Coherent 700 mode-locked tunable dye laser was pumped by an Antares mode-locked Nd:YAG laser. A regenerative Nd:YAG amplifier was used to pump a three stage dye amplifier which produced 1-mJ pulses. The length of the dye laser pulse could be varied from 420 fs to 13 ps. The dye laser beam was circularly polarized and focused to a beam waist of approximately 30-μm diameter at the intersection with the atomic beam. Using a time-of-flight electron energy analyzer we could discriminate between two- and three-photon ionization of the ground state. Alternatively, the population left in the Rydberg states could be detected using field ionization plates. In the latter case, a ramped voltage with a 1-μs risetime was applied to the plates 100 ns after the laser pulse, producing a time-resolved field ionization signal from individual Rydberg states. The electrons produced by both photoionization and field ionization were detected with microchannel plate detectors.

The maximum ac Stark shift was measured by tuning the laser below the two-photon ionization limit by a specific value, such as 100 cm^{-1}, and attenuating the laser while monitoring the production of low-energy electrons. The low-energy electrons were those electrons resulting from two-photon photoionization of the $4s$ ground state. The relative intensity of the laser was monitored using a photodiode. When the peak ac Stark shift was less than 100 cm^{-1}, no production of low-energy electrons was seen since the $4s$ Floquet state did not cross the ionization limit. When the peak ac Stark shift reached the ionization limit, a sharp threshold in the production of low-energy electrons was observed. This threshold provided an accurate intensity calibration of the peak laser intensity. Typical threshold data are shown in Fig. 2 for tunings of 50, 100, and 200 cm^{-1} below the two-photon ionization limit. The data show the ionization signal versus photodiode voltage. From these data we can calculate the peak ac Stark shift in terms of the photodiode voltage to be $\Delta = 363$ cm^{-1}/V. This calibration technique made it unnecessary to measure the minimum beam waist to obtain the peak intensity of the laser pulse. The largest intensity used in the experiment was 7.5×10^{12} W/cm^2, which produced an ac Stark shift of 2000 cm^{-1}.

Figure 3 shows the Rydberg state population after the laser pulse for four different pulse lengths and two laser frequencies, 17 180 and 17 300 cm^{-1}. These tunings correspond to the zero field $4s$ Floquet state being just below the $14d$ and $17d$ states, respectively. The horizontal axis shows the time at which the atoms were field ionized by the ramped voltage so that increasing time corresponds to decreasing values of n. The doublet structure seen at lower n is due to two different m values which ionize at slightly different fields. Although the laser was circularly polarized to produce $l=2$, $m=2$ Rydberg states, the ionizing electric field was orthogonal to the laser propagation direction, which created a superposition of m states. The + symbols represent the calculated Rydberg spectra

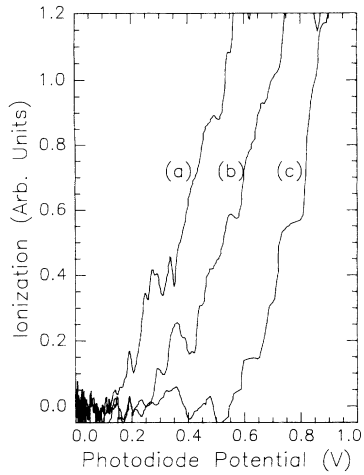

FIG. 2. The low-energy electron signal is shown versus photodiode voltage, which represents the relative intensity of the laser pulses. The tunings for (a), (b), and (c) are 50, 100, and 200 cm^{-1} below the two-photon ionization limit, respectively. The threshold voltage where ionization turns on marks the intensity where the peak ac Stark shift is equal to the detuning from the ionization limit. The threshold intensity increases linearly with detuning.

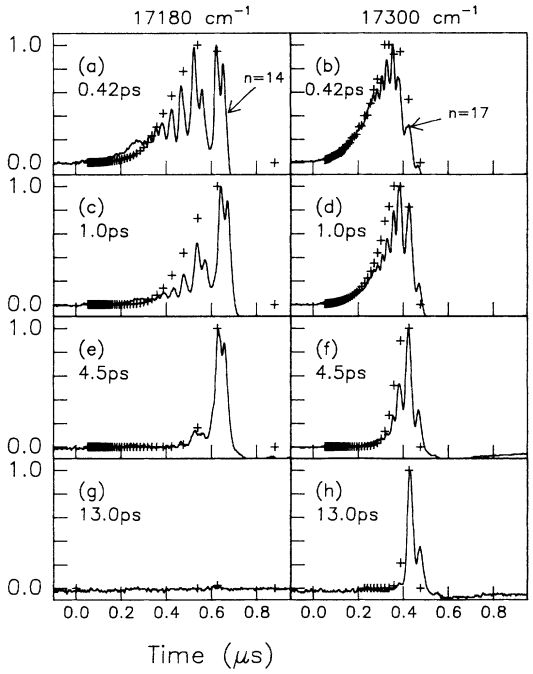

FIG. 3. The residual Rydberg state population detected by field ionization is shown for pulse widths of 0.42, 1.0, 4.5, and 13 ps, with laser frequencies of 17 180 and 17 300 cm^{-1}. The x axis shows the time at which the atoms were ionized by the electric field which was ramped on after the laser pulse. Also shown is the calculated spectra (+). For the 17 180 cm^{-1} tuning in (a), (c), (e), and (g), the zero-field position of the $|4s,2\rangle$ Floquet state is just below the 14d state. For the 17 300-cm^{-1} tuning in (b), (d), (f), and (h), the $|4s,2\rangle$ state is just below the 17d state. The doublet structure is due to different m_1 values which ionize at slightly different fields.

which include averaging over the Gaussian spatial profile of the laser beam. The only adjustable parameter in the calculation was the overall normalization. As can be seen in Fig. 3, the 0.42-ps pulse populated a large range of Rydberg states. This large range is due to the relatively fast passage through the avoided crossings on the rising edge of the pulse, resulting in a small transfer of population to any one state. Even though the transition probabilities to individual Rydberg states during the rising edge of the laser pulse were small, the accumulated effect of the entire Rydberg series produced a dramatic decrease in the ground-state population by the time it reached the ionization limit.

As the pulse length was increased, the final Rydberg state population became more concentrated in the lower n states. For the longer pulses the atoms traversed the first few avoided crossings more adiabatically, which depleted the 4s population and left no atoms to populate higher n states or cross the two-photon ionization limit. The depletion of the 4s state can be seen easily in Fig. 3(e), where population is seen only in the first three states, even though there was sufficient intensity to shift the ground state above the two-photon ionization limit. In this case all the atoms made a transition to the Rydberg states early in the pulse. The data in Fig. 3(g) show the result of a fully adiabatic passage through the anticrossing with the 14d state. In this figure, no population is observed in any Rydberg state. The lack of signal in Fig. 3(g) is not due to low peak intensity; the intensity was sufficient to shift the ground state through three Rydberg state resonances. The lack of population is due to the almost completely adiabatic transitions both from the 4s state to the 14d state on the rising edge of the pulse and from the 14d state back to the 4s state on the falling edge of the pulse, as shown by the arrow in Fig. 1. During the peak of the pulse these atoms were in the 14d state, which was less likely to be photoionized than the ground state. If the coupling to the Rydberg states is reduced, as is the case for the higher tuning in Fig. 3(h), the passage becomes partially diabatic so that population is again seen in the Rydberg states.

In Figs. 4(a), 4(b), and 4(c) we show the low-energy electron yields from two-photon ionization as a function of laser wavelength for pulse durations of 4.5, 1.0, and 0.42 ps, respectively. These signals represent ionization of atoms which did not make a transition to a Rydberg state, but are ionized by two photons from the ground state when it passes above the two-photon limit. In the Figs. 4(a)–4(c), the ionization signal shows a rapid decrease when the laser was tuned below the two-photon ionization limit at 17 505 cm^{-1} and is constant above it. Ionization is observed farthest below the limit for the shortest pulse, for in this case atoms in the 4s Floquet state are more likely to pass diabatically through the avoided crossings with the Rydberg states and be ionized by two photons.

Assuming that the atoms are all initially in the 4s Floquet state, we have calculated the two-photon ionization spectra for the three pulse lengths of Figs. 4(a), 4(b), and 4(c). The results, which include spatial averaging, are shown by the solid lines in Figs. 4(a), 4(b), and 4(c). The

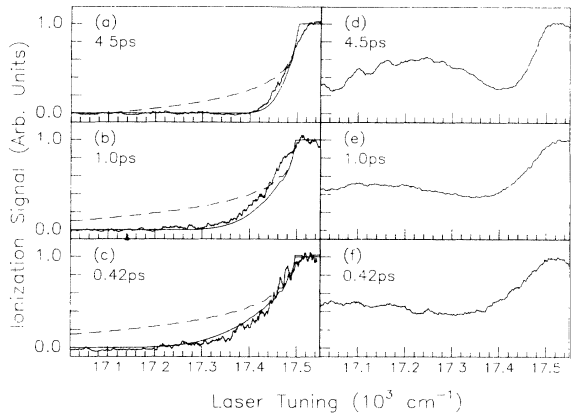

FIG. 4. The photoionization signal for 4.5-, 1.0-, and 0.42-ps pulse lengths versus frequency tuning of the laser, 17 505 cm^{-1} being the two-photon ionization limit. (a), (b), and (c) are the two-photon ionization signals. The rough curves are the data, the smooth solid curves are the calculated spectra which includes transitions to the Rydberg states and the dashed curves are a calculation which neglects the Rydberg state interaction. (d), (e), and (f) show data of the total ionization signal including the photoionization of the Rydberg states. The maximum shift at the peak of the pulse for the three pulse times is 800, 1600, and 2000 cm^{-1} for the 4.5-, 1.0-, and 0.42-ps pulses, respectively.

only adjustable parameter in the calculation is the overall normalization. As can be seen in Fig. 4, the signal agrees well with the calculation. We have also performed the calculation assuming a purely diabatic traversal of the Rydberg states (dashed line), ignoring the possibility of population transfer to the Rydberg states. This assumption leads to the prediction of a larger two photon photoionization yield, which does not agree with the data. The effect is more pronounced for longer pulse times where the passage through the Rydberg anticrossings is slower, resulting in increased population transfer to the Rydberg states.

Figures 4(d), 4(e), and 4(f) show the total photoionization signal, i.e., the sum of two-photon ionization and three-photon ionization via the Rydberg states, as a function of laser wavelength for 4.5-, 1.0-, and 0.42-ps pulse lengths. The pronounced minimum in Fig. 4(d) is due to the population being trapped in high Rydberg states which have a low rate of photoionization, due to the n^{-3} scaling of the photoionization cross section. For the shorter pulses the minimum is less pronounced but still present.

A broad range of experimental data shows unambiguously a marked dependence on the pulse length of the laser. The excellent agreement between the data and calculations based on the dynamic Floquet model show that it gives an accurate description of the evolution in a laser pulse over a substantial range of pulse lengths.

IV. CLOSELY SPACED STATES AND CONTINUITY AT THE IONIZATION LIMIT

In Sec. II, we showed that the coupling V_n, between the 4s and nd Floquet state was proportional $n^{-3/2}$. For isolated avoided crossings between the 4s and nd states, the minimum separation between the two Floquet states is V_n. However, since the coupling decreases less rapidly for increasing n than the spacing between states, which is equal to n^{-3} in atomic units, the assumption of isolated avoided crossings is not valid for all n. This situation is shown in Fig. 5 for a laser tuning of 17 300 cm^{-1}, for which the zero field 4s Floquet state lies just below the 17d state. In Fig. 5 both the coupling (solid line) and the spacing between adjacent n states (dashed line) are shown versus n. The spacing between states falls off as n^{-3}. The coupling initially increases, since higher intensity is necessary to shift the 4s state into resonance with the higher n states, reaches a maximum at $n=25$ and then falls off as $n^{-3/2}$ above $n=25$. At $n=29$ the size of the coupling is equal to the spacing between states and above this state, the coupling is larger than the spacing between states.

The significance of this situation can be seen in Fig. 6, which shows the diagonalized adiabatic Floquet energy levels (in terms of the binding energy) versus the laser intensity. The dotted line represents the energy of the 4s state excluding the interaction with the nd states. The isolated avoided crossings can be easily seen for the lowest n state. However, where the 4s Floquet state intersects the higher n states, the energies of a number of nd states are perturbed for any given laser intensity; i.e., the 4s Floquet state is interacting with many n states simultaneously. For the highest n states, the presence of the 4s Floquet state is difficult to discern. In this regime, which we shall refer to as the strong-coupling regime, many Rydberg states are coupled together via the interaction with the ground state. The composition of the diagonalized states in the strong-coupling regime is a mixture of the ground state and many Rydberg states. The ground-state character is spread among many of the

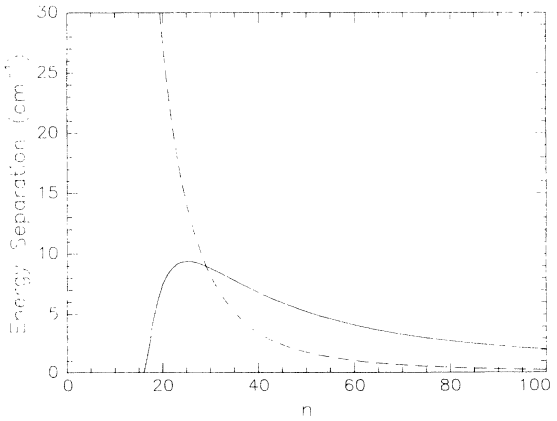

FIG. 5. The coupling between the nd Rydberg states and the 4s Floquet states is shown (solid line) versus n for a laser tuning of 17 300 cm^{-1}, so that the zero-field 4s Floquet state is located just below the energy of the 17d state. The initial increase in coupling is due to the increased intensity needed to shift the 4s state into resonance with the higher Rydberg states. The eventual decrease in coupling is due to the $n^{-3/2}$ dependence of the coupling strength. Also shown is the spacing between Rydberg states (dashed line) which has a n^{-3} dependence.

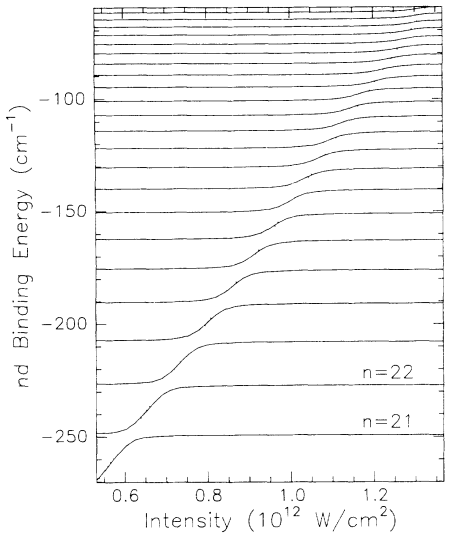

FIG. 6. The diagonalized Floquet energy levels, in terms of binding energy, are shown versus the binding energy of the diabatic 4*s* Floquet state for a laser tuning of 17 300 cm^{-1}. The *nd* states range from $n=21$ to 42. For low-n states the avoided crossings are well isolated. For the high-n states the 4*s* Floquet state interacts with many Rydberg states simultaneously. The dotted line represents the trajectory of the 4*s* Floquet state without interaction with the Rydberg states.

diagonalized Floquet states. The interaction between the ground state and all the Rydberg states in this regime is approximately equal, which causes the position of the Floquet states to "lock" at the energy of $-1/2(n+1/2)^2$. The locking is due to the equal repulsion from the neighboring state above and below. The shift of $0.5n^{-3}$ is due to the inclusion of an extra state, the 4*s* Floquet state, in the Rydberg series. The locking of energy levels occurs whenever a series of states are strongly coupled through a state outside of the series. The locking of Rydberg states has been shown in the strong-coupling region in atomic collisions [23] and in the coupling of Rydberg states via one-photon interaction with the continuum [24].

The transition probabilities due to overlapping avoided crossings have been investigated previously for their importance in atomic collisions [25]. A theoretical result of this work is that the probability of a system's remaining in the initial diabatic state after traversing a sequence of avoided crossings is the same whether or not the avoided crossings overlap. In other words Eq. (8), which gives the population in the ground state after traversing many isolated avoided crossings, is valid even if the avoided crossings are not isolated but overlapping [26].

In the Appendix we show explicitly that the transition probability from the initial state to a sequence of final states is the same if the avoided crossings are isolated or if all the final states are degenerate. We then present qualitative arguments as to why the degeneracy of the states is not critical to the result.

To test the prediction that the Landau-Zener formula applies irrespective of whether or not the avoided level crossings are isolated, we have examined the population remaining in high n states where the avoided crossings are overlapped, as shown in Fig. 6. Figure 7 shows field ionization data versus time, taken for four tunings of the laser. For the four tunings of Fig. 7, the laser pulse was 4 ps (FWHM), and the peak ac Stark shift of the 4*s* Floquet state was 175 cm^{-1}. The top of the figure shows the corresponding n values of the data. The relationship between the time and the n states can be found using the time dependence of the electric field, which increases as t^3 over the range of the data shown, and the n dependence of the field ionization, given by $E_n=1/16n^4$, which gives the relationship $n \propto t^{-3/4}$. At these values of n we cannot resolve individual Rydberg states. However, one can see that the signal initially increases with increasing n, due to the increasing intensity needed to shift to higher n states, reaches a maximum, and then decreases as n increases.

The Landau-Zener calculation, shown by the dotted line, includes spatial averaging and reproduces the data very well. The only adjustable parameter in the calculation is the overall normalization. The normalization between calculations for different tunings was not adjusted. The agreement between the data and the calculation demonstrates that the simple Landau-Zener transition model accurately describes the population transfer between the 4*s* Floquet state and the excited states even in the strong-coupling regime.

It has been shown theoretically and experimentally that the Landau-Zener transition probability can be used to describe transitions to bound states, even if the avoided crossings are overlapping. We now show theoretically that this method may be extended across the ionization limit, to give the energy distribution of the ejected electrons.

Consider a group of Rydberg levels which span an en-

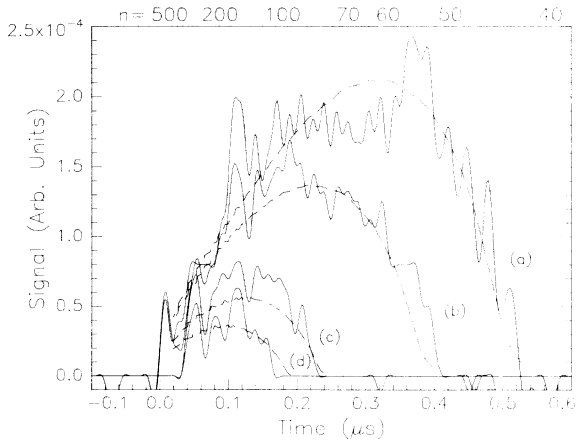

FIG. 7. The field ionization signal (solid curve) versus time is shown for four tunings of the laser with the tunings of (a), (b), (c), and (d) being 60, 40, 19, and 13 cm^{-1} below the two photon ionization limit, respectively. The upper x axis shows the corresponding n values. The simulated spectra (smooth curve) which was calculated using Landau-Zener transitions is in good agreement with the data.

ergy range ΔW as shown by Fig. 6. If we are interested in the total transition probability from the ground state to these levels, how many levels there are and their precise arrangement are unimportant. Only the sum of the squared coupling matrix elements, $\sum V_n^2$ plays any role. Using Eq. (A9) from the Appendix we can write P_g, the probability of the atom's remaining in the ground state after traversing the N avoided crossings as

$$P_g = \exp\left[\frac{-2\pi\sum V_n^2}{dw/dt}\right], \tag{22}$$

and the probability of finding the atom in one of the N Rydberg states is given by

$$P_N = 1 - P_g . \tag{23}$$

Equivalently, P_N gives the transition probability to states of final energy between W and $W+\Delta W$. An important point to remember is that it is unimportant whether there are ten or one thousand states in the energy range ΔW if only $\sum V_n^2$ enters into the transition probability.

We ultimately wish to find the transition probability into final states in the energy range ΔW. First, we convert the sum of Eq. (22) to an integral over the energy range ΔW using

$$\begin{aligned}\sum V_n^2 &= \frac{d\sum V_n^2}{dn}\frac{dn}{dW}\Delta W \\ &= V_n^2 n^3 \Delta W .\end{aligned} \tag{24}$$

For energies just below the ionization limit the squared matrix element V_n^2 exhibits a $1/n^3$ scaling, as described previously. Explicitly,

$$V_n^2 = A(E) n^{-3} . \tag{25}$$

For the two-photon process we have described, $A(E) \propto E^4$. V_n^2 is the squared matrix element per state. It can be converted to the squared matrix element per unit energy, V_E^2, by multiplying by the density of states $dn/Dw = n^3$,

$$V_E^2 = \frac{d\sum V_n^2}{dW} = V_n n^3 = A(E) . \tag{26}$$

When expressed as a squared matrix element per unit energy V_E^2 passes smoothly across the ionization limit, so we can write the transition probability from the initial state to the N states over an energy ΔW as

$$P_N = 1 - \exp\left[\frac{-2\pi V_E^2 \Delta W}{dW/dt}\right], \tag{27}$$

irrespective of whether the energy is above or below the limit. The equivalence of bound and continuum states comes from the fact that V_n only depends on the small r part of the Rydberg or continuum wave function.

Equation (27) gives a transition probability to the states in the energy range ΔW. This energy range is crossed in a time Δt, and dividing Eq. (27) by Δt and taking the limit $\Delta t \to 0$ gives the ionization rate above the limit. Taking the limit $\Delta t \to 0$, $\Delta W/\Delta t = dW/dt$ and Eq. (27) reduces to the ionization rate

$$R_{g\to N} = 2\pi V_E^2 , \tag{28}$$

which is simply Fermi's golden rule, since V_E^2 is the squared matrix element between the initial state and a continuum state normalized per unit energy. At any energy the rate at which electrons are ejected is simply given by the photoionization rate at that energy and laser intensity. In a more general way, we can use Eq. (28) to describe the excitation to the final states in an energy range ΔW irrespective of whether they are bound or free.

Because of the small shifts in our experiment, we cannot resolve the energy spectrum of the electrons which undergo two-photon ionization. However, field ionization provides high resolution of the energies of the Rydberg states. We can rescale the field ionization signal in terms of binding energy to compare the data to our calculation. By rescaling the data, we are treating the high Rydberg states as continuum states in which the number of electrons produced per unit energy is the desired information. The rescaled data of Fig. 7 are shown in Fig. 8 along with a calculation for the population per unit energy. The field ionization data are cutoff at the ionization limit, whereas the calculation extends to the maximum shift of 175 cm^{-1}. The data are in excellent agreement with the calculation. As in Fig. 7, the only adjustable parameter is the overall normalization. The calculated spectra in Fig. 8 are identical for all of the laser tunings except for the energy offset due to different starting points. The spectra are the same because the interaction per unit energy does not change over the range of the experiment. The shape of the energy spectra comes from the coupling which is increasing with intensity and the spatial volume which decreases with increasing peak intensity.

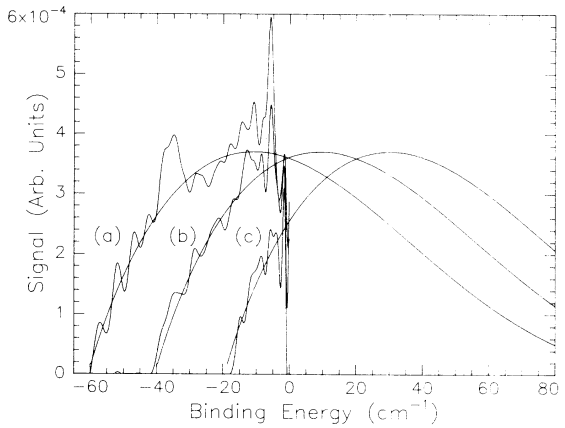

FIG. 8. The two-photon excitation signal per unit energy is shown versus binding energy for three tunings of the laser with (a), (b), and (c) being 60, 40, and 19 cm^{-1} below the two photon ionization limit, respectively, with a laser pulse of 4-ps duration and a maximum ac Stark shift of 175 cm^{-1}. The data (rough line) cuts off at the ionization limit since we only detect electrons left in Rydberg states. Up to the ionization limit, the data shows excellent agreement with the calculated spectra (smooth line). The calculation for the three tunings is identical except for the shift in energy position.

The calculation shown in Fig. 8 does not include the possibility of the populations returning to the ground state during the falling edge of the pulse. When the two-photon transition is to the continuum, after excitation the electrons move away from the atom so that during the falling edge of the pulse there is no possibility of making an adiabatic transition back to the ground state. The same is true for the high Rydberg states which have long classical orbit periods. Even though the Rydberg electrons eventually return to the core, for Rydberg states above $n=30$, which has a classical orbit period of 4 ps, the laser pulse is over before the return. For low-n states, with well separated avoided crossings, such as the case in Fig. 2, we can treat the wave functions as individual stationary states. For the intermediate n Rydberg states, $n \approx 30$, the return of the wave packet during the laser pulse should be considered. For the data shown in Fig. 8, the lowest Rydberg state populated is $n=43$ so that we can neglect the return of the wave packet.

Using Eq. (27) we can calculate the ionization probability per unit energy for a single peak intensity, without the complication of spatial averaging. This calculation is shown in Fig. 9 for a 4-ps laser pulse with various peak ac Stark shifts of the 4s Floquet state ranging from 100 to 220 cm^{-1}. The zero-field position of the 4s Floquet state is at zero binding energy (at the ionization limit). For the lowest peak intensities, the probability of ionization is greatest near the peak shift because of the slow rate of change of the energy of the 4s state near the peak of the laser pulse. Near the peak of the laser pulse, the second derivative of the energy correction of Eq. (10) must be included. For the highest peak intensities, the probability falls off before reaching the peak of the laser pulse. This decrease in ionization probability is due to depletion of the ground-state population before reaching the temporal peak of the laser pulse. For higher peak intensities the ionization probability spectrum does not change. Virtually all atoms are ionized before the 4s Floquet state reaches a shift of 220 cm^{-1}. A model which includes the spatial variation of the laser pulse intensity such as the one used to generate Fig. 8 is made up of many diagrams such as the ones in Fig. 9. The diagrams are scaled by the appropriate spatial volume and added together with a cutoff at the peak intensity at the center of the laser beam.

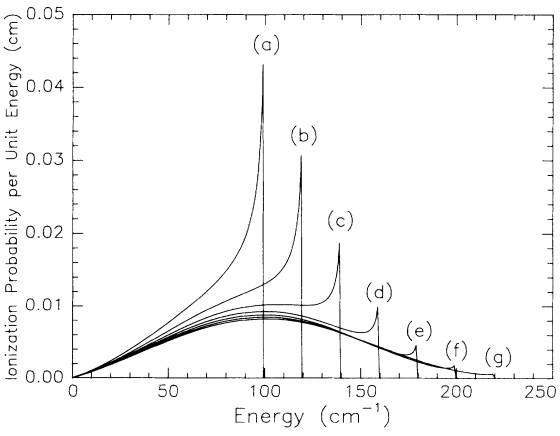

FIG. 9. The calculated ionization probability per unit energy is shown versus energy for pulses with peak ac Stark shifts of (a), (b), (c), (d), (e), (f), and (g) being 100, 120, 140, 160, 180, 200, and 220 cm^{-1}, respectively. These calculations do not include spatial averaging. For the lowest intensity pulses, sharp cusps are seen at the peak ac Stark shift due to the slow rate of change of the energy of the 4s Floquet state near the peak of the laser pulse. The highest intensity pulses show depletion of the ground state during the rising edge of the pulse.

To observe the spectrum in Fig. 9 experimentally, a laser with a large beam waist interacting with atoms in a small interaction region would be required to remove the spatial volume effect. The small interaction region can be achieved with a small aperture of the atomic beam along with a small collection hole. The requirement on the laser power to achieve large shifts without focusing is a much more difficult obstacle to overcome. However, by using high-resolution field ionization of Rydberg states as opposed to energy analysis of free electrons, small shifts due to relatively weak laser fields can be detected which may allow the observation of single peak intensity effects.

This analysis suggests that photoionization can be viewed as a continuous series of Landau-Zener transitions. The advantage of this view is that it predicts the energy distribution of the photoionized electrons and predicts the depletion of the ground state during the rising edge of the laser pulse. In this view of photoionization, a "short" pulse is defined as a pules which does not saturate the photoionization during the rising edge of the pulse, so that the largest contribution to the ionization signal comes from the peak of the pulse producing a cusp such as the one seen in Fig. 9(a). The calculation shown in Fig. 9(g) which has the same pulse duration (4 ps) would not be considered a short pulse since the photoionization is saturated during the rising edge of the pulse. So the determination of whether a pulse is "short" depends not only on the pulse duration but also on the peak intensity. As the peak intensity increases, the pulse duration must be shortened to remain in the short-pulse regime.

V. CONCLUSION

We have observed the population of Rydberg states of K via two-photon intensity-tuned resonances with the ground state during the rising edge of laser pulses of varying pulse lengths. We have found that the resultant spectra depend strongly on the pulse length because of the change in the rate at which the resonances are traversed. The population of Rydberg states was found to have a profound effect on the photoionization probability due to depletion of the ground-state population and the relatively small cross section for photoionization of the high Rydberg states. A dynamic Floquet model which treats the intensity-tuned resonances as avoided crossings of the Floquet states gives excellent agreement with the data. The Floquet model is found to be valid in the strong-coupling regime where the 4s Floquet states interacts with many Rydberg states simultaneously. Because the high Rydberg states evolve smoothly into the

continuum, these states provided a test of the extension of the Floquet model into the continuum to predict the energy spectrum of photoelectrons.

ACKNOWLEDGMENTS

This work was supported by the National Science Foundation. It is a pleasure to acknowledge helpful discussions with R. R. Jones and J. B. Delos.

APPENDIX

The limiting case of closely spaced states is a system with N degenerate excited states. This case is instructive in understanding the strong-coupling regime and will be described in detail here. The Hamiltonian for this system can be written as

$$H = H_0(t) + V(t) \tag{A1}$$

where H_0 has $N+1$ eigenvectors $|g\rangle$ and $|n\rangle$ where n runs from 1 to N with

$$H_0|g\rangle = \omega_g|g\rangle \tag{A2}$$

and

$$H_0|n\rangle = \omega_n|n\rangle \ . \tag{A3}$$

For the degenerate case ω_n is the same for all n. $V(t)$ is the interaction between the ground state and the excited states. We start with the general time-dependent wave function

$$|\psi(t) = C_g(t)\exp\left[-i\int_0^t \omega_g dt'\right]|g\rangle + \sum_n^N C_n(t)\exp\left[-i\int_0^t \omega_n dt'\right]|n\rangle \ , \tag{A4}$$

where C_g is the time-dependent coefficient of the dressed ground state and C_n is the time-dependent coefficient of the excited states. The time-dependent wave function is inserted into the Schrodinger equation,

$$H|\psi(t)\rangle = i\frac{d|\psi(t)\rangle}{dt} \ , \tag{A5}$$

giving a set of $N+1$ coupled differential equations,

$$i\frac{d}{dt}C_g = \tfrac{1}{2}\exp\left[i\int_0^t \omega\, dt'\right]\sum_n^N V_n C_n \tag{A6}$$

and

$$i\frac{d}{dt}C_n = \tfrac{1}{2}\exp\left[-i\int_0^t \omega\, dt'\right]V_n C_g \ , \tag{A7}$$

where ω is the energy difference between the dressed ground state and the excited states and V_n is the coupling between the ground state and the nth excited state. In the degenerate case we can decouple the ground-state equation resulting in a second-order differential equation for C_g. Explicitly,

$$\frac{d^2}{dt^2}C_g - i\omega\frac{d}{dt}C_g + \tfrac{1}{4}\sum_n^N V_n^2 C_g = 0 \ . \tag{A8}$$

The form of this equation is exactly the form of a single anticrossing [21] with V^2 replaced by $\sum_n^N V_n^2$. Using the Landau-Zener formalism we can immediately write the solution for the final ground-state population

$$P_g = \exp\left[-\frac{2\pi\sum_n^N V_n^2}{d\omega/dt}\right] = \prod_n^N \exp\left[-\frac{2\pi V_n^2}{d\omega/dt}\right] \ , \tag{A9}$$

which is the same result as would be obtained from passing through N isolated anticrossings. So the final ground-state population is independent of whether the anticrossings are traversed simultaneously or as a sequence of isolated two-level avoided crossings.

[1] P. Kruit, J. Kimman, H. G. Muller, and M. J. van der Wiel, Phys. Rev. A **28**, 248 (1983).
[2] H. G. Muller, A. Tip, and M. J. van der Wiel, J. Phys. B **16**, L679 (1983).
[3] P. Agostini, P. Breger, A. L'Huillier, H. G. Muller, and G. Petiet, Phys. Rev. Lett. **63**, 2208 (1989).
[4] R. R. Freeman, P. H. Bucksbaum, H. Milchberg, S. Darack, D. Schumacher, and M. E. Geusic, Phys. Rev. Lett. **59**, 1092 (1987).
[5] M. P. de Boer and H. G. Muller, Phys. Rev. Lett. **68**, 2747 (1992).
[6] R. B. Vrijen, J. H. Hoogenraad, H. G. Muller, and L. D. Noordam, Phys. Rev. Lett. **70**, 3016 (1993).
[7] J. G. Story, D. I. Duncan, and T. F. Gallagher, Phys. Rev. Lett. **70**, 3012 (1993).
[8] M. C. Baruch and T. F. Gallagher, Phys. Rev. Lett. **68**, 3515 (1992).
[9] D. G. Papaioannou and T. F. Gallagher, Phys. Rev. Lett. **69**, 3161 (1992).
[10] P. Agostini and L. F. DiMauro, Phys. Rev. A **47**, R4573 (1993).
[11] G. N. Gibson, R. R. Freeman, and T. J. McIlrath, Phys. Rev. Lett. **69**, 1904 (1992).
[12] T. J. McIlrath, R. R. Freeman, W. E. Cooke, and L. D. van Woerkom, Phys. Rev. A **40**, 2770 (1989).
[13] C. E. Moore, *Atomic Energy Levels,* Natl. Bur. Stand. (U.S.) Circ. No. 467 (U.S. GPO, Washington, DC, 1949).
[14] M. V. Federov, in *Multiphoton Processes,* edited by G. Mainfray and P. Agostini (CEA, Saclay, France, 1991), p. 89.
[15] B. Sundaram and L. Armstrong, J. Opt. Soc. Am. B **7**, 414 (1990).
[16] K. C. Kulander, K. J. Schafer, and J. L. Krause, Phys. Rev. Lett. **66**, 2601 (1991).
[17] R. R. Jones, D. W. Schumacher, and P. H. Bucksbaum, Phys. Rev. A **47**, R49 (1993).
[18] L. D. Landau, Phys. Z. Sowjetunion **2**, 46 (1932).
[19] C. Zener, Proc. R. Soc. London Ser. A **137**, 696 (1932).

[20] J. R. Rubbmark, M. M. Kash, M. G. Littman, and D. Kleppner, Phys. Rev. A **23**, 3107 (1981).

[21] R. B. Vrijen, J. H. Hoogenraad, and L. D. Noordam, Mod. Phys. Lett. B (to be published).

[22] W. L. Wiese, M. W. Smith, and B. M. Miles, *Atomic Transition Probabilities,* Nat'l. Bur. Stand. Ref. Data Ser., Natl. Bur. Stand. (U.S.) Circ. No. 22 (U.S. GPO, Washington, DC, 1969), Vol. II.

[23] The strong-coupling case was investigated by Demkov and co-workers in atomic collisions. Yu. N. Demkov and I. V. Komarov, Zh. Eksp. Teor. Fiz. **50**, 286 (1966) [Sov. Phys. JETP **23**, 189 (1966)]; Yu. N. Demkov and V. I. Osherov, Zh. Eksp. Teor. Fiz. **53**, 1589 (1967) [Sov. Phys. JETP **26**, 916 (1968)].

[24] In a series of papers Federov and co-workers considered the strong-coupling regime in terms of interference effects in multiphoton excitation and ionization of Rydberg states. M. V. Federov and A. M. Movsesian, J. Opt. Soc. Am. B **5**, 850 (1987); M. V. Federov, M. Y. Ivanov, and P. B. Lerner, J. Phys. B **23**, 2505 (1990); M. V. Federov, M. Y. Ivanov, and A. M. Movsesian, *ibid.* **23**, 2245S (1990) and references therein.

[25] J. B. Delos and co-workers considered the adiabatic and diabatic evolution of atoms during atomic collisions using a discretised continuum. J. B. Delos and W. R. Thorson, Phys. Rev. A **6**, 728 (1972); J. B. Delos, *ibid.* **9**, 1626 (1974); R. D. Taylor and J. B. Delos, Proc. R. Soc. Lond. Ser. A **379**, 209 (1982); T. S. Wang and J. B. Delos, Phys. Rev. A **33**, 3832 (1986) and references therein.

[26] R. G. Hulet and D. Kleppner, Phys. Rev. Lett. **51**, 1430 (1983). The strong coupling between nearest neighbors was investigated in the context of microwave interaction with a Stark state manifold.